CONSTRUCTION
E-ISSN: 2785-8731
VOLUME 6, ISSUE 2, 2026, In-Press
DOI: https://doi.org/10.15282/construction.v6i2.14614

RESEARCH ARTICLE

Inspection-driven service life assessment of corroded steel structures of an electrostatic precipitator building

Nur Ainun Mawaddah, Angga Fajar Setiawan* and Suprapto Siswosukarto

Department of Civil and Environmental Engineering, Faculty of Engineering, Gadjah Mada University, Yogyakarta 55281, Indonesia

Abstract: Corrosion-induced degradation in steel structures exposed to combined coastal–industrial environments presents a critical challenge for long-term structural performance and maintenance planning. This study proposes a field-based, dual-approach framework for evaluating the remaining life of steel structures in an Electrostatic Precipitator (ESP) building of a coal-fired power plant. The assessment includes visual inspection, corrosion mapping, ultrasonic thickness gauge (UTG) measurements, and hardness testing to characterize material deterioration under aggressive environmental conditions. Using a unified field dataset, two complementary approaches are applied: (1) a corrosion-based method following ISO 9224 to estimate Remaining Service Life (RSL) based on thickness loss and corrosion rate, and (2) a condition-based method based on ISO 15686 to estimate Remaining Useful Life (RUL) through condition factors and visual inspection data. The results indicate that corrosion affects all structural elements, with bracing exhibiting the most severe degradation, followed by beams, while columns remain relatively less affected. Beam and bracing elements show higher corrosion rates, greater thickness reduction, and shorter estimated service life compared to columns. The comparison between RSL and RUL demonstrates consistent trends in identifying critical structural components, highlighting the reliability of integrating corrosion-based and condition-based assessments. The proposed framework enables rapid, practical, and data-driven evaluation of structural degradation without requiring detailed structural analysis at the preliminary stage. This approach provides a useful decision-support tool for maintenance prioritization in existing steel structures subjected to aggressive environmental exposure.

Article History
Received : 27 April 2026
Revised : 6 October 2026
Accepted : 8 November 2026
Published : 17 November 2026

Keywords
Atmospheric corrosion
Steel structure
Remaining useful life
Condition assessment
Inspection

1. Introduction

The long-term durability of steel structures remains an important challenge in the management of modern industrial infrastructure, particularly as many facilities continue to operate beyond their initial design life. Steel offers high strength, structural efficiency, and ease of fabrication and construction. However, it is inherently vulnerable to environmental degradation over time. Exposure to atmospheric conditions can initiate corrosion processes that progressively deteriorate material properties and reduce structural performance. This process is influenced by several environmental factors, including temperature, humidity, pH, and air pollutants such as SO_2, H_2S, NO_x, CO_2, dust particles, and sea salt [1], [2]. Gradual corrosion can lead to material degradation, including reductions in effective cross-sectional area, changes in mechanical properties, and a decrease in structural capacity, potentially accelerating the achievement of a Serviceability Limit State before the life of the structure is reached.

The degradation of steel materials is most aggressive in infrastructure in environments with high levels of corrosion. According to ISO 9223 [3], the medium to extreme category generally occurs in coastal environments and industrial areas. The marine atmosphere contains aerosols containing Cl^- ions that can accelerate the corrosion of steel. Meanwhile, industrial atmospheres contain substantial amounts of sulfur dioxide (SO_2), produced by the combustion of coal, oil, and gasoline, which are highly corrosive [4]. Even if the steel has been coated with a protective coating, such as Hot Dip Galvanized (HDG) or Cold Galvanized Coating (CGC), the steel is still susceptible to corrosion. Experimentally, HDG efficiency in extreme environments (CX) reached 25.95%, while CGC in the C4 category reached 74.85%. These findings show that coating only slows degradation, as the corrosion rate remains determined by the degree of environmental aggressiveness [5]. Therefore, steel structures located in a combination of coastal and industrial environments need to be evaluated to assess the feasibility of using their structural components. In these aggressive environments, the impact of corrosion extends beyond material degradation to the performance of structural components. For example, in structural applications, steel dampers rely on their strength and deformation capacity to function effectively under cyclic loading. However, they are susceptible to strength degradation due to buckling and fracture mechanisms [6], which can be further accelerated by corrosion, leading to cross-sectional loss and material deterioration. Therefore, corrosion protection is essential to ensure that steel dampers can maintain their performance throughout their service life.

Various approaches have been employed to evaluate the effect of corrosion on the performance of steel structures. Evaluation of corrosion conditions can be carried out through visual inspection, Ferroxyl testing, measurement of residual material thickness, and electrochemical techniques to identify the level of material degradation [7]. Loss of thickness due to corrosion has also been shown to affect the mechanical properties of steel columns and decrease the ultimate capacity of structural elements [8]. Numerical analysis conducted by Sharifi et al. [9] showed that cross-section reduction due to corrosion was directly correlated with a decrease in the moment capacity of steel beams. Similar findings were reported

*CORRESPONDING AUTHOR | Angga Fajar Setiawan | ✉ angga.fajar.s@ugm.ac.id
© 2026 The Authors. Published by Universiti Malaysia Pahang Al-Sultan Abdullah Press. This is an open access article under the CC BY-NC 4.0 license

by Li et al. [10] and Shu et al. [11], who stated that corrosion degradation can lead to a progressive decrease in the capacity of structural elements over time.

Evaluation of corrosion conditions is important for estimating the remaining useful life (RUL), the time remaining before a component reaches its performance limit. Putra et al. [12] examined steel oil storage tanks using visual inspection and ultrasonic thickness testing, and found uniform corrosion at a rate of 0.034 mm/year, with an estimated remaining life of about 20 years. Meanwhile, Chaerany et al. [13] evaluated a 30-year-old steel frame building in Muara Badak through visual observation, non-destructive testing, static load testing, and numerical analysis. The results show a corrosion rate of about 0.2 mm/year with a deflection of 17 mm, as well as an estimated remaining service life of about 36 years with periodic maintenance and reinforcement. However, most existing studies apply these methods independently and often rely on numerical simulations, limiting their practicality for rapid field-based assessments. Furthermore, many studies focus on individual structural components rather than evaluating multiple elements within an integrated structural system.

This research addresses these limitations by proposing a combined, field-based dual-approach framework for assessing the remaining life of steel structures using a unified dataset. Unlike previous studies that apply these approaches separately or rely on numerical simulations, this research demonstrates how practical field inspection data can be directly utilized to derive consistent and comparable service life predictions. The research focuses on an Electrostatic Precipitator (ESP) building in a coal-fired power plant located in a coastal–industrial environment, which represents a highly aggressive exposure condition. The assessment integrates visual inspection, corrosion mapping, ultrasonic thickness measurements, and hardness testing to characterize material degradation. From the same field data, two complementary methods are applied: a corrosion-based approach using ISO 9224 to estimate remaining service life (RSL) based on corrosion rate and thickness loss over time, and a condition-based approach using ISO 15686 to estimate remaining life based on inspection results and condition factors. By comparing these approaches within the same structural system, this study provides a practical tool for early identification of structural conditions and rapid estimation of remaining service life in power plant facilities, offering a faster and more accessible preliminary evaluation for industrial application.

2. Materials and Methods

2.1 Characteristics of the Research Area

The research was conducted at a Coal-fired Power Plant located on the island of Java, Indonesia, with a generating capacity of 660 MW. The power plant has been in operation since 2016 and is situated in a coastal area characterized by high salinity and exposure to pollutants from coal combustion. This is in line with previous research by Sundjono et al. [14], which found that the coastal area of Java has high salinity. This increases the risk of corrosion, especially due to chloride ions that damage the passive layer of steel and low dissolved oxygen levels. In addition, emissions from burning coal, such as CO_2, SO_2, O_2, and water vapor, increase the relative humidity of the environment, which in turn accelerates the rate of corrosion [15].

2.2 Object

The object of this research is the Electrostatic Precipitator (ESP) building, which consists of a steel structural system combining portal frames and bracing elements. The ESP building is shown in Figure 1. The ESP's structure is designed to withstand gravitational loads from large internal components as well as lateral loads from wind and earthquakes [16]. In aggressive environments, steel elements in the ESP building are susceptible to progressive thickness reduction due to corrosion, particularly in structural members such as columns, beams, and bracing. This degradation reduces the cross-sectional capacity and increases the vulnerability of the structure to instability and failure. Given the critical role of the ESP system in controlling emissions, maintaining its structural integrity is essential for safe and continuous operation.

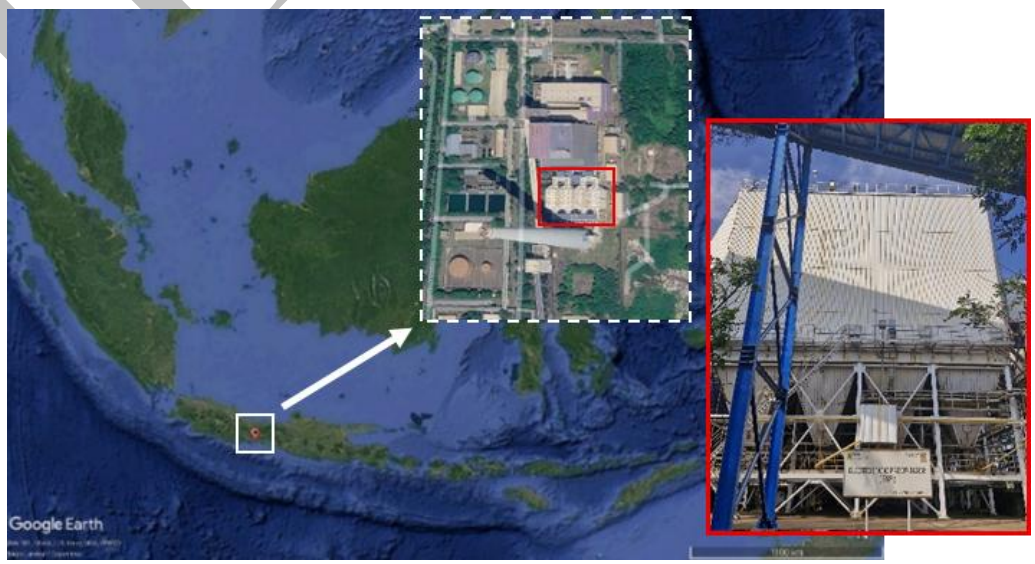


Figure 1. Location and research object (Source: google earth)

2.3 Research Workflow

This section describes in detail the stages and flow of the research, as shown in Figure 2. The research was carried out through three main stages: preparation, data collection, and data analysis. The preparation stage included a literature review and the collection of secondary data, such as as-built drawings of Electrostatic Precipitator (ESP) buildings and maintenance information. The data collection stage involved field inspections, including visual inspection of corrosion levels, hardness testing, and the Ultrasonic Thickness Gauge (UTG) Test. The collected data were then used to develop corrosion mapping and quantify material degradation. In the analysis stage, the remaining service life was estimated using two approaches based on established standards. The corrosion-based approach follows ISO 9224:2012 to determine actual corrosion rates, thickness loss over time, and Reference Service Life, while the condition-based approach applies ISO 15686-8:2008 using the factor method to estimate Remaining Useful Life.

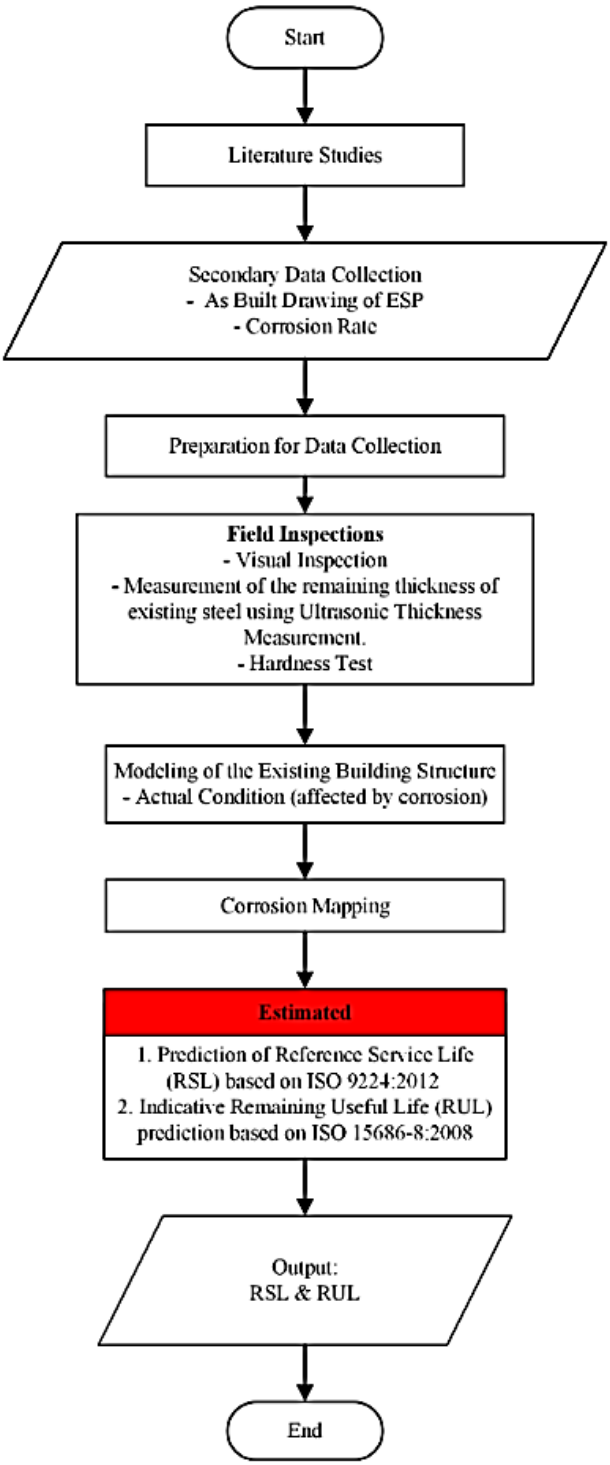


Figure 2. Research stage flowchart

This study presents a preliminary, condition-based assessment framework for estimating degradation and remaining life using field data. The approach focuses on material-level deterioration, where thickness reduction is used as the

primary indicator of corrosion effects, allowing an early-stage evaluation without requiring detailed structural analysis. Nevertheless, thickness reduction implicitly reflects structural capacity loss under assumed constant loading. The estimation of remaining life is based on established standards (ISO 9224 and ISO 15686) and supported by field measurements; however, no direct validation using historical data or long-term monitoring has been conducted. Therefore, the results should be clearly interpreted as indicative estimations based on current conditions and standard-based assumptions, rather than fully validated predictive models.

2.4 Steel Structure Condition Assessment

Condition assessment is carried out to identify the level of material degradation due to corrosion and evaluate the actual condition of the steel structural elements. The assessment process is carried out through the following stages.

2.4.1 Visual inspection

Visual inspection is carried out as an initial stage to identify indications of corrosion on the surface of structural elements. Observations are focused on discoloration of the steel surface, rust formation, damage to the protective layer, and indications of material loss. Condition documentation is carried out through field recording and the capture of photos of degraded elements. Identification of characteristics and levels of corrosion visually refers to the research by Morcillo et al. [5].

2.4.2 Corrosion mapping

Corrosion distribution mapping is performed to identify the location and severity of corrosion on the observed structural elements. Each corroded area is marked and classified based on the degree of surface damage observed. This mapping aims to describe the spatial distribution of corrosion degradation in structural systems, enabling clear identification of areas with higher corrosion levels. Corrosion mapping refers to Table 1 by combining Rust Grade ASTM D160 [17], research by Oyarhossein et al. [18], and research by Morcillo et al. [5].

Table 1. Visual-based steel corrosion index-classification

Severity Level	Colour	Rust Grade ASTM D160 [17]	Visual Indicator [18]	Loss of Thickness [5]	Structural Implications
Very Severe	Red	0-2	Steel is exposed, protective coating completely lost	Significant swelling and layer delamination occur	Risk of local to global failure
High	Orange	3-4	Extensive delamination, partial loss of coating; rust around areas/weld joints	Corrosion size 5–25 mm. Swelling occurs and the coating begins to peel	Reduction in structural capacity
Moderate	Yellow	5-6	Localized pitting corrosion, non-uniform distribution	Corrosion size 1–5 mm and non-uniform	Reduction in local capacity
Light	Green	7-8	Light rust spots, change in coating color, no significant damage	Small corrosion size, early stage	Early degradation, not yet critical
No Corrosion	Blue	9-10	No rust or delamination	None	Does not affect structural performance

2.4.3 Hardness test

Material hardness was tested on several structural elements using a portable hardness tester to determine the mechanical properties of the steel. The results of this test are used to ensure that the material remains within the mechanical properties range specified for the steel structure material. The Hardness Test is shown in Figure 3. The tool used is a Portable Leeb Hardness Tester Type D with an HLD output, and the values were then converted to HB in accordance with ASTM E-140 [19] using Equation (1). To find out the value of ASTM E-140 (2012) Ultimate Tensile Strength/fu, the value of HB was converted to fu (MPa) as shown in equation (2), referring to Pavlina et al. [20].

$$HB = 2.7862E^{2} - 2.3014E^{HLD} + 7.8978E^{-3HLD^{2}} - 9.5946E^{-6(HLD)^{3}} + 5.0641E^{-9(HLD)^{4}} \quad (1)$$

$$TS = 3.45HB \quad (2)$$

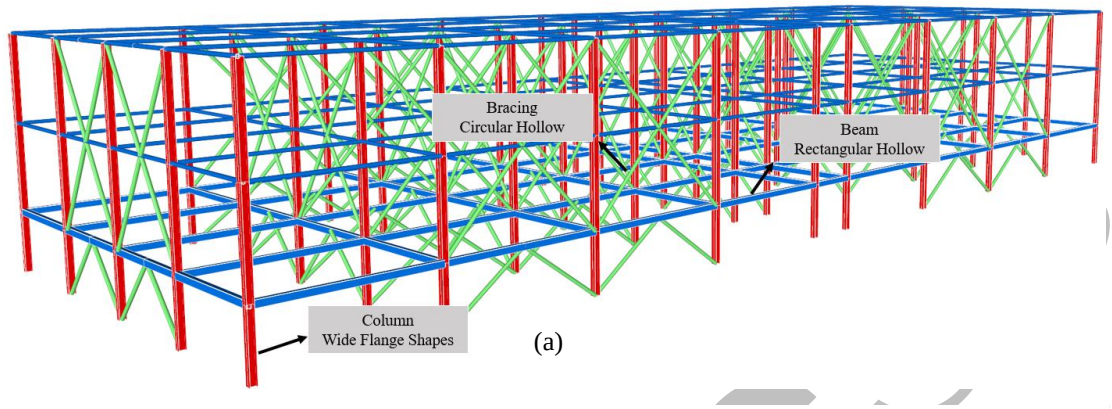
2.4.4 Measurement of element dimensions, existing thickness, and damage dimensions

After secondary data collection, it was found that the as-built drawing for the ESP building was incomplete, so the dimensions of the structural elements were verified by direct measurements of parts of the existing structure in relatively good condition, identified through visual inspection as having minimal corrosion and representing near-intact geometry. This measurement includes the profile dimensions of structural elements such as the height and width of the cross-section, as well as the existing thickness of the cross-section. The measurement locations for the element dimensions are located at Grid A (front area), specifically for column 1-A, beam 4–5 A, and bracing 2–3 A, selected as baseline elements due to their relatively preserved condition. Table 2 shows the details of the profiles and dimensions of the structural elements in the ESP building.

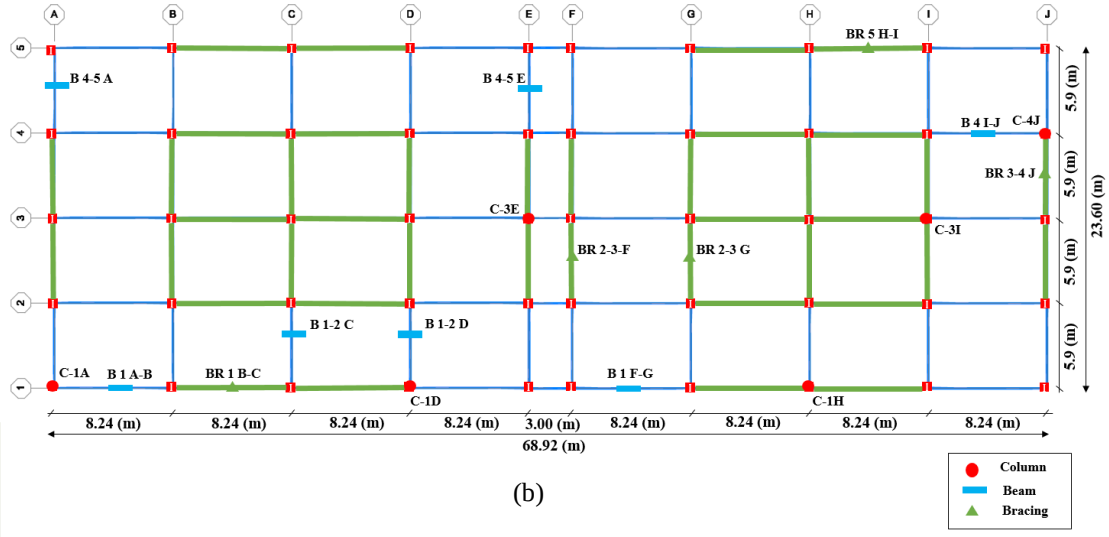
In-Press

Table 2. Profile and dimensions of ESP building structural elements

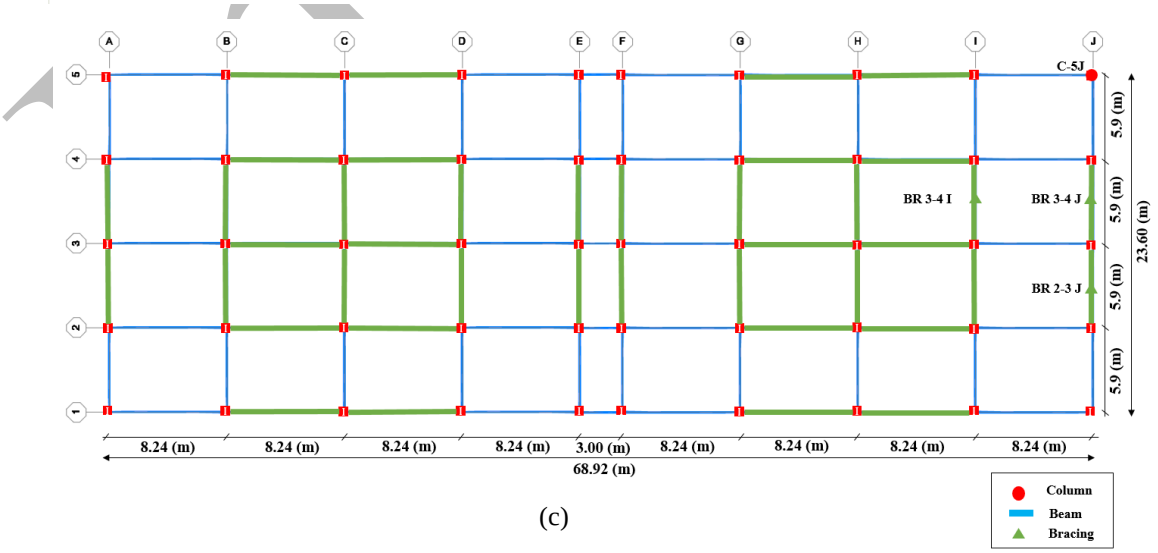
Element	Profile Type	Main Dimensions (mm)	Thickness (mm)	Remarks
Beam	Rectangular Hollow	300 x 200	6	A (Height) x B (Width)
Column	Wide Flange Shapes	300 x 300	Web = 10 Flange = 15	H-shape profile
Bracing	Circular Hollow	D = 170	8	Outer diameter



(a)



(b)



(c)

Figure 3. UTG Locations (a) 3D View of ESP's structural elements; (b) UTG locations 1st floor; (c) UTG locations 2nd floor

The thickness of existing steel elements was measured using an ultrasonic thickness gauge. This measurement is carried out at several observation points that represent the structure's condition to obtain data on the actual thickness of the material, whether on column elements, beams, or bracing. Measurement samples were taken from areas with severe corrosion to capture critical degradation conditions and the maximum extent of thickness reduction. It is acknowledged that the deliberate selection of severely corroded measurement points produce conservative corrosion rate estimates, which are considered appropriate for a preliminary screening assessment but may not be representative of average element conditions. Moreover, the unmeasured areas may exhibit different corrosion conditions that are not fully characterized by the selected measurement points. In addition, the selection of measurement points also considered accessibility and safety constraints during field inspection, which are common in assessments of existing structures. Measurements were therefore carried out at locations that were both accessible and representative of the observed corrosion conditions. The measurement process is shown in Figure 4. The UTG testing locations are shown in Figure 3, and the tests were conducted on the 1st floor and 2nd floors. In addition, in areas that have experienced severe corrosion to the point of perforation or holes, direct damage dimensions are measured to identify the area and shape of the cross-sectional loss. The actual thickness data and damage dimensions are used to identify the level of material loss due to corrosion and serve as the basis for the corrosion rate analysis, as well as for the estimation of the remaining service life of the structure at the next stage of analysis.



(a) (b) (c)

Figure 4. Existing thickness measurements of ESP building (a) column; (b) beam; (c) bracing

2.5 Estimate Remaining Service Life (RSL) Based on Corrosion Rate

The remaining life of the structure is estimated based on the cross-sectional reduction of structural elements due to corrosion. The cross-sectional reduction of structural elements due to corrosion is modeled by reducing the steel element thickness based on the corrosion rate determined from field measurements. The change in the thickness of the element over time is expressed in Equation (3). This equation is used to simulate the cross-sectional degradation of steel elements over time, as described in the model of steel structure degradation by Melchers et al. [21]. The corrosion rate is calculated from the material thickness loss over exposure time using Equation (4), where CR is the corrosion rate (mm/year), t_0 is the initial thickness according to the standard, t is the existing thickness of the measurement result, and T is the exposure time. This equation refers to the atmospheric corrosion evaluation approach described in ISO 9224: 2012 and to the corrosion literature by Fontana [22].

Calculation of the remaining life of the structure uses the Critical Thickness Profile (CTP) approach to evaluate the distribution of thickness loss and potential for further degradation. Thus, a critical thickness is obtained as a structurally safe minimum limit as well as the basis for estimating a conservative Remaining Service Life (RSL) according to the actual conditions of Equation (5). The critical thickness concept ($t_{critical}$) is the minimum element thickness that still meets the performance criteria based on cross-sectional capacity. In this study, the determination of critical thickness is guided by the fitness-for-service principles in API 579-1/ASME FFS-1, which provide a general framework for assessing structural feasibility under corrosion degradation. However, a detailed fitness-for-service or structural capacity assessment is beyond the scope of this study, and a detailed structural capacity analysis is not performed. Therefore, the critical thickness is not considered a definitive structural failure or serviceability limit, but rather a practical threshold for preliminary screening. The selection of the threshold is supported by previous studies demonstrating that progressive section loss can significantly reduce the capacity of steel members. Palanivelu et al. [23] reported that exposure to aggressive acidic environments, such as H_2SO_4, resulted in approximately 30–38% thickness loss within a relatively short period and was accompanied by a noticeable reduction in mechanical capacity. Although the corrosion environment in that study differs from the atmospheric corrosion conditions considered herein, the findings provide supporting evidence that substantial thickness loss can be associated with measurable deterioration in material performance. In addition, Sharifi and Rahgozar [9] reported a reduction in the remaining moment capacity of corroded steel beams with increasing flange and web thickness loss, while their study on shear capacity showed that a 25% web thickness loss can cause a significant reduction in the remaining shear capacity. Furthermore, a recent study on corroded H-section steel columns reported that a 37% area loss resulted in a 43–51% reduction in ultimate and buckling loads [24], which is directly relevant to the wide-flange columns considered in this study. Collectively, these studies indicate that section losses in the range of approximately 20–30% can result in substantial reductions in moment capacity, shear capacity, compressive strength, and buckling resistance in different types of steel members. Based on this evidence, a critical thickness retention range of 70–80% of the initial thickness is adopted as a conservative screening threshold in this study. This range is therefore used as a practical indicator of significant cross-sectional degradation for condition-based assessment and RSL estimation, rather than as a directly validated structural capacity limit.

$$t = t_0 - (CR\ X\ T) \tag{3}$$

$$CR = \frac{t_0 - t}{T} \tag{4}$$

$$RSL = \frac{t_{actual} - t_{critical}}{CR} \tag{5}$$

2.6 Indicative Remaining Useful Life Estimate

Indicative Remaining Useful Life (RUL) estimation uses a service-life planning approach that refers to the concept of Reference Service Life (RSL) and the Factor Method-based correction method outlined in the standard ISO 15686-8:2008 [25]. In this ISO, Residual Service Life (RSL) is defined as the reference life of components at the reference use condition (design life) minus the used life (age), as shown in Equation (6). In addition to RSL, Remaining Useful Life (RUL) is also formulated as the residual indicative life, which is calculated from the value of RSL multiplied by the multiplier factor A-F, shown in Equation (7). Based on ISO 15686-8:2008, the multiplier factor can be modified according to the representation of actual conditions in the field. This is emphasized the study by Ad Straub [24] and Potrc Obrecht et al. [25], where the value of factors is greatly influenced by various parameters such as environment, design, and maintenance. Therefore, the factor needs to be calibrated and adjusted to the actual conditions to make the estimated service life more representative. Factor modifications are shown in the Table 3.

$$RSL\ (year) = Design\ Life - Age \tag{6}$$

$$RUL = RSL\ X\ A\ X\ B\ X\ C\ X\ D\ X\ E\ X\ F \tag{7}$$

Table 3. Modified factor values refer to ISO 15686-8:2008 and field conditions

Factor	Parameter	Range	Basis for selection
A	Material Quality	0.90 – 1.00	Structural Steel - Standard
B	Structural Design	0.80 – 0.90	Design with many joints, potential water traps, and dust accumulation
C	Construction	0.90 – 1.00	Good Construction
D	Environment	0.60 – 0.85	Environmental aggressiveness in coastal and industrial areas
E	Service Conditions	0.90 – 1.00	Relatively normal loads, exposure to coal combustion pollutants
F	Maintenance	0.75 – 0.90	Maintenance is performed routinely, but not comprehensively across all elements

3. Results and Discussion

3.1 Visual Inspection & Corrosion Mapping Results

Visual inspection of existing buildings is conducted to assess corrosion conditions in the steel structures of ESP buildings. The assessment focuses on identifying the severity and distribution of corrosion using visual indicators, such as rust intensity, surface degradation, and potential cross-sectional reduction. It is noted that the steel surfaces were previously painted approximately one year ago, which may influence the current visual appearance of corrosion. The recent repainting is considered to have negligible effect on UTG measurements as the instrument was calibrated to read steel substrate thickness; however, it may have partially obscured early-stage surface corrosion during visual inspection, potentially causing mild underestimation of light-category corrosion. The results of the corrosion classification are visually presented in the corrosion mapping for each structural element, shown in Figure 5. Details of the corrosion visualization of each category are presented in Figure 6. Corrosion mapping refers to Table 1.

Based on Figure 6, the types of corrosion in the beam elements are identified as crevice corrosion at the beam-column connection, pitting corrosion, and uniform corrosion on the beam's cross-sectional surface. For column elements, the type of corrosion found is uniform corrosion on the flange area, causing thickness reduction. Meanwhile, for the bracing element, pitting corrosion was identified that developed into perforation in both the bracing-column and bracing-beam connection areas.

After identifying and mapping the corrosion level for all elements of the ESP building structure, the distribution of corrosion levels was quantified. The elements that have a certain degree of corrosion dominance, including the light category, and those that have reached critical conditions, were identified. The distribution of corrosion rates is shown in Figure 7. The graph shows that column, beam, and bracing elements are all dominated by moderate-level corrosion, with the highest values in columns (52%), followed by bracing (45%) and beams (32%). The bracing element is the most critical because it has the highest proportion of very severe levels (30%), while the beam shows a relatively even distribution between moderate and high levels. Meanwhile, columns tend to experience moderate corrosion, with the lowest proportion of very severe (8%). Overall, there are no uncorroded elements, indicating that the entire structure has undergone varying degrees of degradation.

UMP Press

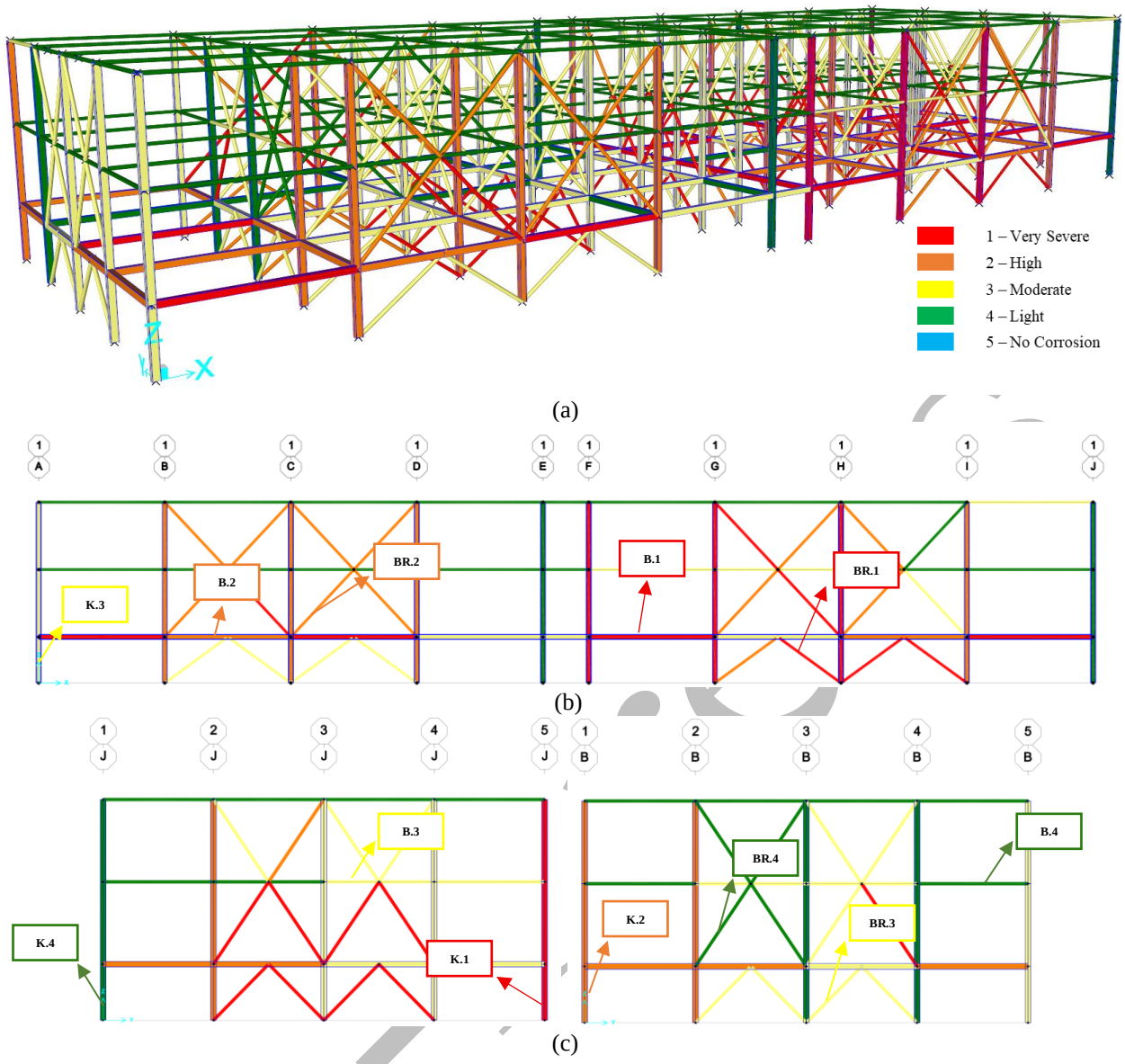


Figure 3. Corrosion mapping Of the ESP building steel structure (a) Mapping of corrosion levels; (b) Detailed mapping of the corrosion level in the x-axis direction; (c) Detailed mapping of the corrosion level in the y-axis direction



B.1 – Very Severe
(Perforation 4-7 cm)

B.2 – High
(Perforation 2-3 cm)

B.3 – Moderate
(Pitting Corrosion)

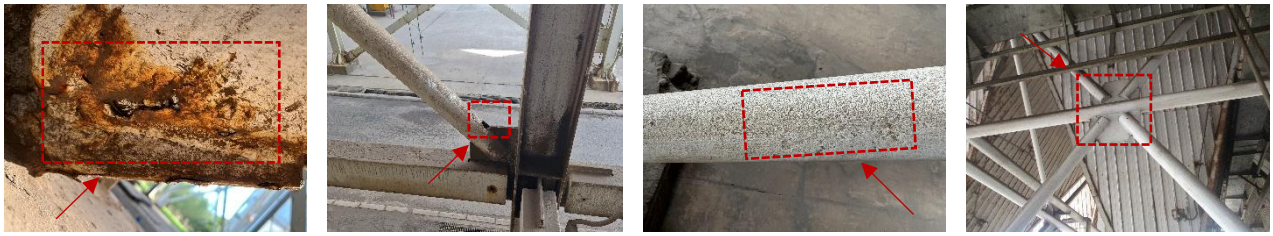
B.4 – Light
(Rust spots & coating degradation)

(a)



K.1 – Very Severe (Perforation 4-7 cm) | K.2 – High (Perforation 2-3 cm) | K.3 – Moderate (Pitting Corrosion) | K.4 – Light (Rust spots & coating degradation)

(b)



BR.1 – Very Severe (Perforation 4-7 cm) | BR.2 – High (Perforation 2-3 cm) | BR.3 – Moderate (Pitting Corrosion) | BR.4 – Light (Rust spots & coating degradation)

(c)

Figure 4. Visualization of the corrosion level of steel structure of ESP buildings (a) Beam; (b) Column; (c) Bracing

The observed higher corrosion severity in bracing elements can be attributed to their geometric configuration and exposure conditions. Bracing members are typically more slender and are often located in positions that facilitate moisture accumulation, pollutant deposition, and limited drainage, which accelerate localized corrosion such as pitting. In addition, their connection details may create crevice conditions that further intensify corrosion mechanisms. Compared to columns, which are generally more robust and less exposed to water trapping, bracing and beam elements are therefore more vulnerable to accelerated degradation.

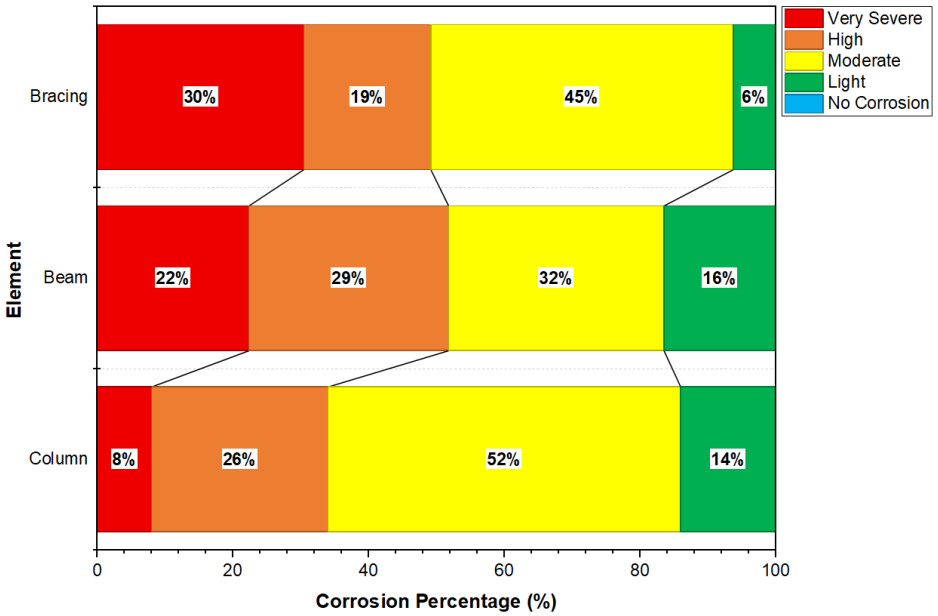


Figure 5. Corrosion level distribution of ESP building

During the visual inspection, several perforations were identified in beam and bracing elements, as shown in Figure 8. Measurements indicate that perforations in bracing members range from 3–10 cm in diameter with lengths up to 17 cm, while beam elements exhibit smaller perforations with lengths of 1–5 cm and widths of 1–4 cm. The greater severity of corrosion observed in bracing elements is likely associated with their geometric configuration and exposure conditions. Compared to columns, which are generally more robust and less susceptible to water trapping, bracing and beam elements are therefore more vulnerable to accelerated degradation. These perforations are attributed to the progression of pitting corrosion; as reported by Sun et al. [26] & Liu et al. [27], pitting can propagate through the thickness of steel plates due to its high growth rate, ultimately leading to perforation. This indicates that the observed damage likely originated from localized pitting and evolved into more advanced material degradation.



(a) BR 2-3 G 1st floor; (b) BR 3-4 F 1st floor; (c) BR 2-3 H 1st floor; (d) BR 3-4 G 1st floor



(e) BR 5 B-C 1st floor; (f) BR 5 G-H 1st floor; (g) BR 5 H-I 1st floor; (h) BR 5 H-I 2nd floor

(a)



(a) B 1-2 C 1st floor; (b) B 1 A-B 1st floor; (c) B 5 F-G 1st floor; (d) B 1 I-J 1st floor



(e) B 4 F-G 1st floor; (f) B 1-2 H 1st floor; (g) B 2 H-I 1st floor; (h) B 4 I-J 2nd floor

(b)

Figure 6. Perforation on (a) bracing; (b) beam

3.2 Hardness Test Results

The hardness test results reveal a noticeable degradation in the mechanical properties of the steel material after approximately 10 years of operation. Hardness testing is performed at several sample points representing the structural elements of columns, beams, and bracing. The results of the hardness test are shown in Figure 9. Based on the graph in Figure 9, the tensile strength of the column elements ranges from approximately 385.25 MPa to 614.1 MPa, with several values falling below the specified range for Q345B steel, indicating partial material degradation. A more significant reduction is observed in beam elements, where tensile strength values decrease to approximately 272–291 MPa, which is below the standard range for Q235B steel. This suggests that beam elements have experienced substantial deterioration in material properties. Meanwhile, bracing shows a high variation (±250–580 MPa), with values below and above the standard, indicating non-uniform material conditions. In general, columns show a reduction in mechanical properties; beams show the most significant degradation; and bracing shows the greatest variation in material condition. It is noted that portable Leeb hardness measurements on corroded surfaces are subject to elevated scatter due to surface roughness and irregularity. The high variation observed in bracing elements may therefore reflect both genuine material non-uniformity and measurement uncertainty inherent to the field instrument. Accordingly, the hardness test results are interpreted qualitatively as corroborative evidence of material deterioration rather than as precise measurements of mechanical properties.

The results of this hardness test are consistent with the research of Lu & Luo [28], which found that corrosion decreases hardness by 40-50% in aggressive environments and directly contributes to increased material damage. A similar result was also found by Shojai et al. [29], who reported that corrosion decreased the material's hardness. The steel's hardness decreased from about 180 HV to 140 HV, indicating a degradation of mechanical properties due to microstructural damage. The observed reduction in hardness and tensile strength is consistent with previous studies indicating that corrosion can lead to microstructural damage and a decrease in mechanical performance. The more pronounced degradation in beams and bracing elements further supports the findings from visual inspection, highlighting that these elements are more severely affected by corrosion than columns. This consistency between material testing and visual assessment strengthens the reliability of the field-based evaluation approach.

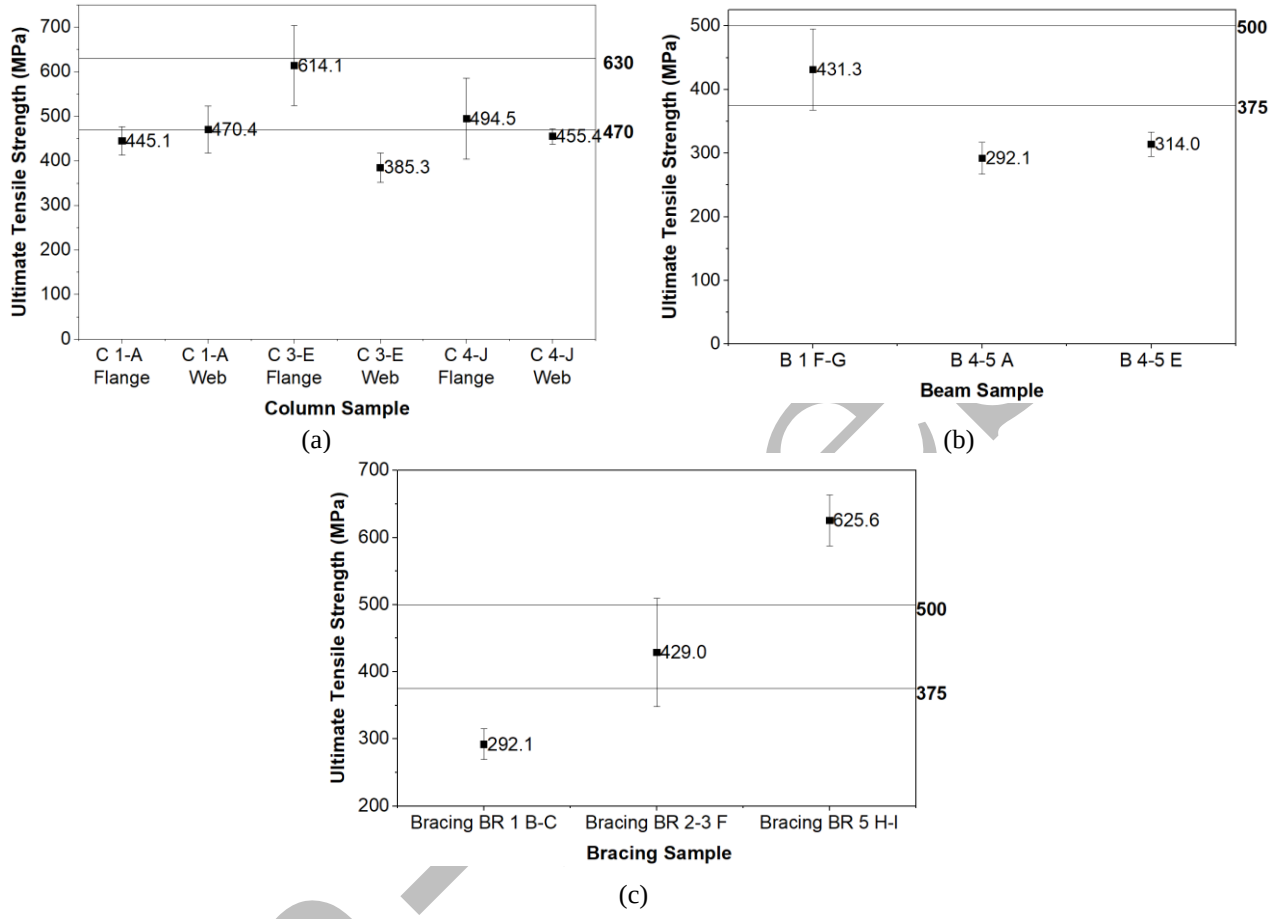


Figure 7. Hardness test results (a) Column; (b) Beam; (c) Bracing

3.3 Existing Thickness Measurement Results

The results of the existing thickness measurements show significant thickness variations in some structural elements, which indicates cross-sectional loss due to corrosion. The non-uniform thickness distribution indicates that degradation is local and influenced by environmental conditions and the position of elements in the structure. To clarify the distribution of these thicknesses, the measurement results are presented as graphs for each element in Figure 10. Thus, the areas with the highest depletion rates can be identified and used as a basis for evaluating the remaining life.

The UTG results of each element are compared to the design thickness as per Table 2. The UTG results indicate significant variability in the remaining thickness of structural elements, reflecting non-uniform corrosion patterns. Several column samples show minor reduction in thickness, with the flange area reduced to 13.28–14.60 mm and the web area to 3.02–9.30 mm. While other samples exhibit values close to or slightly above the design thickness due to the presence of residual coatings or corrosion products during measurement. In contrast, beam elements show consistent thickness reduction, with most samples experiencing a decrease to approximately 3.00–5.86 mm, indicating substantial material loss. Bracing elements exhibit the most severe degradation, with all samples showing thickness reduction below the design specification, ranging from 3.78–7.32 mm. In some samples, a high standard deviation was observed, indicating that corrosion in the bracing was non-uniform.

This reduction in steel thickness is in accordance with the study by Vera et al. [30], where there is a loss of steel thickness at three years of exposure, with an average of 85 μm. The research by Nie et al. [31] also found a reduction in steel thickness over time due to corrosion exposure, which is represented as an increase in corrosion depth from 144 μm to 278 μm. The non-uniform distribution of thickness loss suggests that corrosion is highly localized and influenced by environmental exposure and structural detailing. Areas with higher exposure to moisture and pollutants tend to exhibit

more severe degradation. This finding is consistent with the visual inspection results, where localized pitting and perforation were predominantly observed in beam and bracing elements.

3.4 Estimated Reference Service Life (RSL) Based on Corrosion Rate

The estimated Reference Service Life (RSL) is calculated based on the reduction in the existing thickness and the corrosion rate, as described by Equations (3), (4), and (5). The RSL calculation for each element sample is presented in Figure 10. To represent the overall condition of the ESP building, Table 4 summarizes both the average RSL for each element type and the minimum RSL, which corresponds to the elements experiencing the most severe corrosion conditions. Based on Table 4, the minimum RSL for the column elements, both in the flange and web sections, is 19 years. For the web, the value of 19 years is selected instead of 1 year, as it is considered more representative of the overall condition of all sampled elements. One web sample yielded an anomalously low RSL of 1 year, attributed to a highly localised measurement point; this outlier was excluded in favour of the next minimum value of 19 years as more representative of the element group as a whole. In contrast, the minimum RSL values for the beam and bracing elements are significantly lower, at 3 and 2 years, respectively. This is also illustrated in Figure 10, which shows that the beam and bracing elements undergo greater reductions in thickness than the column elements. These differences are consistent with the visual inspection results.

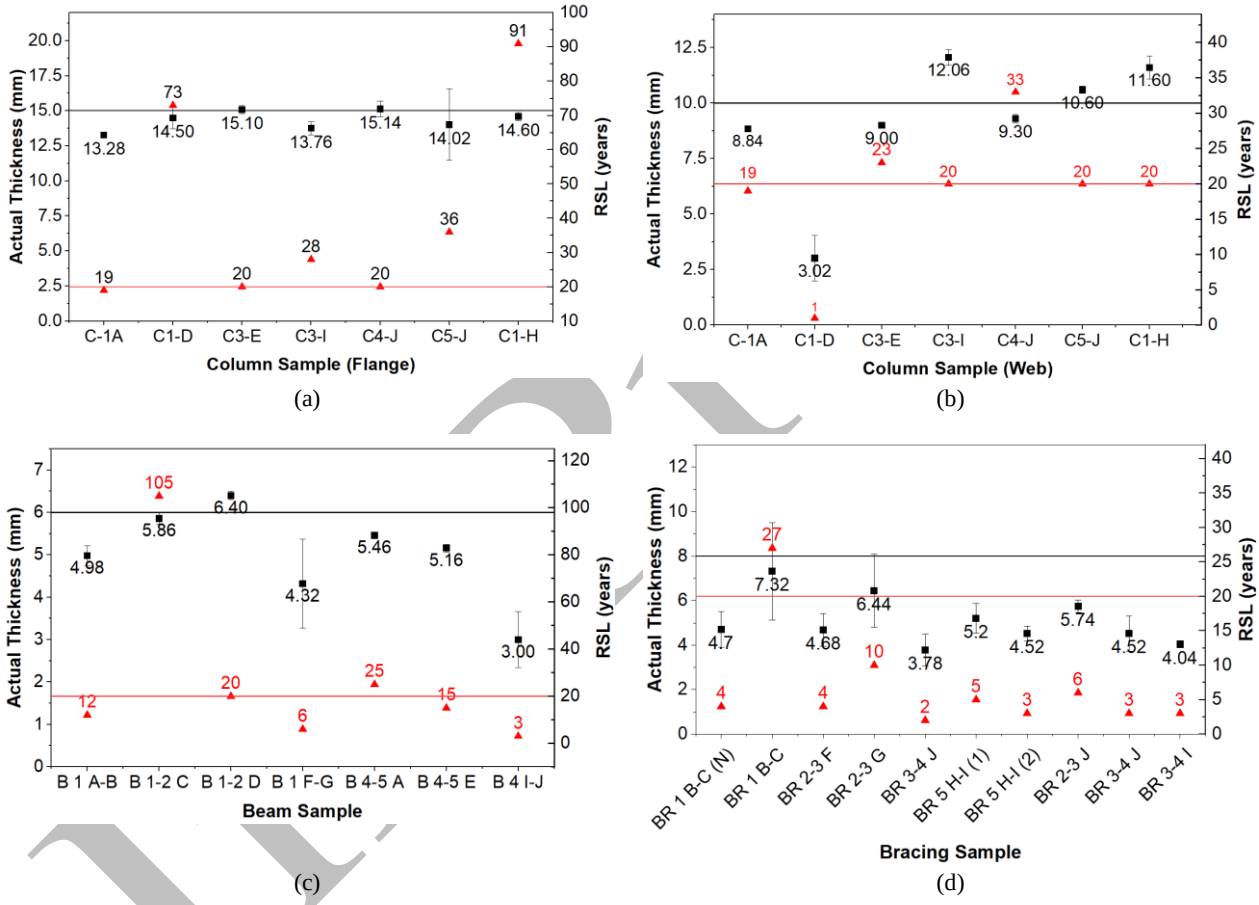


Figure 8. UTG test and RSL results (a) Column-flange; (b) Column-web; (c) Beam; (d) Bracing

The column elements predominantly exhibit uniform corrosion, which leads to gradual thinning and progresses at a relatively slower rate due to a lower corrosion rate. In contrast, the beam and bracing elements are affected by localized pitting corrosion that has developed into perforation, accompanied by higher corrosion rates, resulting in more severe and localized material loss. Therefore, using minimum RSL values is more appropriate for identifying critical structural components and prioritizing maintenance actions. This approach provides a conservative estimation that better reflects the actual risk of structural failure. To clarify the calculation procedure, an example of the Reference Service Life (RSL) calculation is presented as follows:

$$\text{RSL} = \frac{13.28 - 9.96}{0.17} = 19.30 \approx 19 \text{ years}$$

Table 4. Estimation of remaining service life based on corrosion rate

Element	Reference Service Life (years)	
	Minimum (Worst Condition)	Average
Column (Flange)	19	49
Column (Web)	19	17
Beam	3	28
Bracing	2	7

3.5 Indicative Remaining Useful Life (RUL) Estimate

The research was conducted when the ESP building had been in operation for 10 years, since 2016. Based on the design data, the ESP building was originally planned for 20 years[1]. The Indicative Remaining Useful Life (RUL) is calculated in accordance with ISO 15686-8:2008 using the factor method (A-F), which is modified to reflect actual field conditions. Table 5 shows the results of the RUL calculations for each group of structural elements in the ESP building, based on Equation (7). The results indicate that RUL of the column is 3.27 years, while the beam and bracing elements have slightly lower values of 3.08 years. This difference is primarily influenced by the B factor (Structural Design), where the columns are treated differently from the beams and bracing. Based on visual inspection, the design configuration of beams and bracing tends to promote dust accumulation and water trapping, which accelerates corrosion compared to columns. This observation is supported by Figure 8, which shows that very severe corrosion level reaches 22% in beams and 30% in bracing elements, whereas only 8% of column elements fall into this category.

The analysis also shows that the estimated RSL obtained using the corrosion rate approach (Table 4) is generally comparable to the RUL values adjusted for environmental factors (Table 5). The RSL reflects variations among elements due to differences in exposure conditions and corrosion susceptibility. The relatively close values between the two estimates, particularly for the most critical elements, suggest that the assumptions used for corrosion coefficients and environmental factors are reasonably consistent with the observed field conditions. However, it should be noted that both approaches are based on different assessment principles, and the similarity in results does not imply direct equivalence but rather indicates converging estimations under the given assumptions. To demonstrate the calculation procedure, an example of the Remaining Useful Life (RUL) calculation is given below:

$$\text{RSL (year)} = 20 \text{ years} - 10 \text{ years} = 10 \text{ years}$$

$$\text{RUL} = 10 \text{ X } 0.95 \text{ X } 0.85 \text{ X } 1 \text{ X } 0.60 \text{ X } 0.90 \text{ X } 0.75 = 3.27 \approx 3 \text{ years}$$

Based on the estimated RUL, the structural elements of the ESP building are not expected to meet the intended design life. Therefore, several solutions are required to control further corrosion degradation and ensure the structure reaches its target service life. The initial treatment of corroded elements involves applying a recoating system in accordance with ISO 12944 (2017) [34], with the coating system selected based on the environmental corrosivity category. In highly aggressive environments (C5/CX), a high-durability multi-coat system is required, typically consisting of a zinc-rich primer, epoxy intermediate layer, and polyurethane topcoat, along with proper surface preparation through abrasive blasting to ensure adequate adhesion and long-term performance. A similar approach was highlighted by Price and Figueira [35], who emphasized that effective corrosion control can be achieved through advanced protective systems and periodic inspections.

However, in cases where corrosion has resulted in flange thinning in columns and perforation in beams and bracings, an evaluation of the residual structural capacity is required, followed by appropriate structural interventions. Referring to AISC Design Guide 16 [36], recommended repairs include local strengthening methods, such as plate welding or steel jacketing for columns, as well as partial or full replacement of members in critical connection areas for beams and bracing elements. This is because damage in these zones can significantly reduce stiffness and load-carrying capacity [37]. Furthermore, implementing *condition-based maintenance* (CBM) and *risk-based maintenance* (RBM) is essential to effectively prioritize repair actions and extend the structure's overall service life [38]. A more comprehensive structural assessment, including load-carrying capacity evaluation, numerical modelling, and validation with historical or long-term monitoring data, is recommended for future work.

Table 5. Indicative remaining useful life (RUL) estimate

Element	Design Life	Age of the Building	RSL (Reference Service Life)	Factor						RUL
	(years)	(years)	(years)	A	B	C	D	E	F	(years)
Column	20	10	10	0.95	0.85	1	0.60	0.90	0.85	3.27
Beam	20	10	10	0.95	0.80	1	0.60	0.90	0.85	3.08
Bracing	20	10	10	0.95	0.80	1	0.60	0.90	0.85	3.08

[1] Based on the Power Plant's As-Built Drawing, the ESP building was originally designed for a 20-year service life.

3.6 Sensitivity Analysis of RSL and RUL Predictions

Given the variability in the measured corrosion rates and the uncertainty associated with the selected input factors, a sensitivity analysis was performed to evaluate their effects on the estimated Reference Service Life (RSL) and Remaining Useful Life (RUL). For the RSL, the corrosion rate (CR) of the bracing element was varied by ±20% from the actual value to evaluate the effect of changes in the corrosion rate on the predicted service life. For the RUL, the lower and upper bounds of Factors A–F presented in Table 3 were applied to assess the influence of uncertainty in the selected factor values. The baseline condition represents the values used in the main RSL and RUL calculations. The resulting variations in RSL and RUL are presented in Table 6.

The sensitivity analysis shows that the predicted RSL of the bracing element is sensitive to variations in the corrosion rate, with the RSL decreasing from 2.24 years at the baseline condition to 1.87 years when the corrosion rate increases by 20%, while a 20% reduction in the corrosion rate increases the RSL to 2.80 years. For the RUL estimation, varying Factors A–F within their lower and upper bounds results in RUL values ranging from 2.62 to 6.89 years, compared with the baseline value of 3.08 years. These results demonstrate that both corrosion-rate variability and uncertainty in the selected factors can substantially affect the predicted service life, highlighting the importance of considering input uncertainty when interpreting the RSL and RUL estimates.

Table 6. Sensitivity analysis of RSL and RUL

Analysis	Condition	Input/Variation	Estimated Life (years)
RSL – Bracing	CR -20%	0.8 X CR	2.80
RSL – Bracing	Baseline	Actual CR	2.24
RSL – Bracing	CR +20%	1.2 X CR	1.87
RUL	Lower Bound	Minimum values of factors A-F	2.62
RUL	Baseline	Assumed values of factors A-F	3.08
RUL	Upper Bound	Maximum values of factors A-F	6.89

4. Conclusions

This study presents a field-based, dual-approach framework for evaluating corrosion-induced degradation and estimating the remaining life of steel structures in aggressive coastal-industrial environments. The results confirm that corrosion has significantly affected all structural elements of the ESP building, with bracing and beam elements experiencing the most severe degradation, while columns remain relatively less affected. The corrosion pattern further shows a progression from localized pitting to perforation in both bracing and beam elements, suggesting that the deterioration process has reached an advanced stage. The integration of visual inspection, ultrasonic thickness measurements, and hardness testing provides a consistent and reliable representation of material deterioration. The analysis shows that localized corrosion mechanisms, particularly pitting and perforation, play a dominant role in accelerating degradation in slender and exposed elements. Overall, beams and bracing are identified as the most critical elements in the structural system being assessed.

These findings are further reflected in the remaining service life estimation, where both RSL and RUL analyses indicate a clear performance gap between structural elements, with beams and bracing showing significantly shorter remaining life compared to columns. The estimated remaining service life (RSL) from the corrosion rate approach is generally consistent with the remaining useful life (RUL) after applying environmental and other influencing factors. The closeness between the two estimates, especially for critical elements, indicates that the adopted corrosion coefficients adequately represent both material characteristics and environmental conditions. Therefore, the proposed framework produces internally consistent results across two complementary assessment methods. However, external validation against structural capacity data or long-term monitoring is still required and remains a subject for future work. The framework can therefore provide supporting information for service life evaluation and maintenance decision-making.

The estimated Remaining Useful Life (RUL) indicates that the current condition of ESP structural elements is below their intended design life, highlighting the need for additional measures to mitigate further corrosion. An initial step involves applying a suitable recoating system tailored to the environmental conditions, particularly the use of high-durability coatings in highly aggressive environments. In cases of advanced corrosion, such as flange thinning and perforation, structural actions including local strengthening or replacement of critical members become necessary due to their impact on structural performance. In addition, the adoption of condition-based and risk-based maintenance approaches plays an important role in effectively prioritizing repairs and extending the overall service life of the structure. A more comprehensive structural assessment, including load-carrying capacity evaluation, numerical modelling, and validation with historical or long-term monitoring data, is recommended for future work.

Acknowledgements

The authors would like to express their sincere gratitude to Universitas Gadjah Mada for the support provided through an internal research grant, as well as for the facilities and academic environment that enabled this study. The authors also appreciation to the management and technical personnel of the coal-fired power plant for their cooperation, access to the site, and the valuable information shared during the research.

UMP Press

Funding
This research was funded by the Department of Civil and Environmental Engineering, Faculty of Engineering, Universitas Gadjah Mada, through a research grant. The authors would like to express their sincere gratitude to all parties who provided support and contributed to the successful completion of this research.

Declaration of Competing Interests
The authors declare no conflicts of interest.

Credit Author Contribution Statement
Nur Ainun Mawaddah (Conceptualization, data collected, data analysis, writing original draft)
Angga Fajar Setiawan (Conceptualization, data analysis, writing – review and editing)
Suprapto Siswosukarto (Writing – review and editing)

Availability of Data and Materials
The data supporting this study's findings are available on request from the corresponding author.

Ethics Statement
This study did not involve human participants or animals. Ethical approval was therefore not required.

Generative Artificial Intelligence Disclosure
During the preparation of this manuscript, the authors used ChatGPT and Grammarly to improve language clarity and readability. The authors reviewed and edited the content as needed and take full responsibility for the final version of the manuscript.

References
[1] Z. Ahmad, *Principles of Corrosion Engineering and Corrosion Control*, IChemE Series. Butterworth-Heinemann is an imprint of Elsevier, 2006. [Online]. Available: www.icheme.org.
[2] J. Ken and B. Balangao, "Corrosion of Metals: Factors, Types and Prevention Strategies," *Journal of Chemical Health Risks*, vol. 14, no. 1, pp. 79–87, 2024, [Online]. Available: www.jchr.org
[3] ISO 9223, "Corrosion of metals and alloys — Corrosivity of atmospheres — Classification, determination and estimation," 2012.
[4] A. Ul-Hamid, H. Saricimen, A. Quddus, A. I. Mohammed, and L. M. Al-Hems, "Corrosion study of SS304 and SS316 alloys in atmospheric, underground and seawater splash zone in the Arabian Gulf," *Corrosion Engineering Science and Technology*, vol. 52, no. 2, pp. 134–140, Feb. 2017, doi: 10.1080/1478422X.2016.1213974.
[5] T. O. J. Silaban *et al.*, "Types, Mechanisms, and Efficiency Rate of Galvanized Steel as Corrosion Protection in Atmospheric Corrosion: A Systematic Review," *Journal of the Civil Engineering Forum*, pp. 201–216, Mar. 2026, doi: 10.22146/jcef.22512.
[6] A. F. Setiawan *et al.*, "Cyclic Behavior of Multidirectional Box-Shaped Shearing Damper: Experimental Study," *Journal of the Civil Engineering Forum*, vol. 11, no. 2, pp. 203–216, May 2025, doi: 10.22146/jcef.14550.
[7] M. Morcillo, I. Díaz, H. Cano, B. Chico, and D. de la Fuente, "Atmospheric corrosion of weathering steels. Overview for engineers. Part II: Testing, inspection, maintenance," Oct. 20, 2019, *Elsevier Ltd*. doi: 10.1016/j.conbuildmat.2019.06.155.
[8] Q. Zhang, J. Wen, Q. Han, H. Zhuge, and Y. Zhou, "Life-cycle assessment and prediction on ultimate capacity of corroded Q690 steel columns with H-section under bi-directional cyclic loading," *Thin-Walled Structures*, vol. 195, Feb. 2024, doi: 10.1016/j.tws.2023.111391.
[9] Y. Sharifi and R. Rahgozar, "Simple Assessment Method to Estimate the Remaining Moment Capacity of Corroded I-Beam Sections," *Transaction A: Civil Engineering*, vol. 17, no. 2, pp. 161–167, 2010.
[10] M. Li, M. Lei, J. Li, and G. Li, "Prognosis analysis of strength of H-beams considering corrosion effects," in *IOP Conference Series: Earth and Environmental Science*, Institute of Physics Publishing, Feb. 2019. doi: 10.1088/1755-1315/218/1/012082.
[11] Q. Shu, K. Wang, G. Yuan, Y. Zhang, L. Lu, and Z. Liu, "Assessing capacity of corroded angle members in steel structures based on experiment and simulation," *Construction Building Materials*, vol. 244, May 2020, doi: 10.1016/j.conbuildmat.2020.118210.
[12] M. B. P. Putra, J. W. Soedarsono, M. Mahendra, Banarwoto, and M. Ghufran, "Remaining Life Assessment and Corrosion Rate on Storage Tank Using ASME/FFS-1 A 579," *International Journal of Engineering Trends and Technology*, vol. 71, no. 1, pp. 340–348, Jan. 2023, doi: 10.14445/22315381/IJETT-V71I1P230.
[13] A. Chaerany, A. Awaludin, H. Priyosulistyo, and A. Triwiyono, "Structural Condition Assessment of Steel-Framed Maintenance Plant in Muara Badak, Balikpapan, East Kalimantan," *Applied Mechanics and Materials*, vol. 845, pp. 344–355, Jul. 2016, doi: 10.4028/www.scientific.net/amm.845.344.
[14] Sundjono, G. Priyotomi, L. Nuraini, and S. Prifiharni, "Corrosion Behavior of Mild Steel in Seawater from Northern Coast of Java and Southern Coast of Bali, Indonesia," *Journal Engineering Technology Science*, vol. 49, pp. 780–784, 2017, doi: 10.5614/j.eng.technol.sci.2017.49.6.5.

UMP Press

[15] R. Spörl *et al.*, "Mercury and SO3 emissions in oxy-fuel combustion," in *Energy Procedia*, Elsevier Ltd, 2014, pp. 386–402. doi: 10.1016/j.egypro.2014.11.041.
[16] X. Wang, B. Li, and Z. Yang, "Finite Element Analysis and Lightweight Optimization Design on Main Frame Structure of Large Electrostatic Precipitator," *Advances in Materials Science and Engineering*, vol. 2018, 2018, doi: 10.1155/2018/4959632.
[17] ASTM International, "Designation: D 610-01 Standard Test Method for Evaluating Degree of Rusting on Painted Steel Surfaces 1," 2001. [Online]. Available: www.sspc.org.
[18] M. A. Oyarhossein, G. Sugiyama, F. Rodrigues, and H. Rodrigues, "Colour-Coded BIM Models for Corrosion Severity Assessment in Steel Bridges," *CivilEng*, vol. 6, no. 4, p. 67, Dec. 2025, doi: 10.3390/civileng6040067.
[19] ASTM International, "ASTM E-140 - Standard Hardness Conversion Tables for Metals: Relationship among Brinell Hardness, Vickers Hardness, Rockwell Hardness, Superficial Hardness, Knoop Hardness, Scleroscope Hardness, and Leeb Hardness," 2012.
[20] E. J. Pavlina and C. J. Van Tyne, "Correlation of Yield strength and Tensile strength with hardness for steels," *Journal of Materials Engineering and Performance.*, vol. 17, no. 6, pp. 888–893, Dec. 2008, doi: 10.1007/s11665-008-9225-5.
[21] R. E. Melchers and R. J. Jeffrey, "Probabilistic models for steel corrosion loss and pitting of marine infrastructure," *Reliability Engineering and System. Safety*, vol. 93, no. 3, pp. 423–432, Mar. 2008, doi: 10.1016/j.ress.2006.12.006.
[22] M. G. . Fontana, *Corrosion engineering*. McGraw-Hill, 1987.
[23] S. Palanivelu, S. Avudaiappan, and N. Maureira-Carsalade, "Corrosion behaviour of mild steel in diverse environments: a comparative study of hot-rolled and cold-rolled specimens," *Journal of King Saud University - Engineering Sciences*, vol. 37, no. 6, Oct. 2025, doi: 10.1007/s44444-025-00038-2.
[24] Q. Xue, S. Xu, A. Li, and Y. Wang, "Local–overall buckling behavior of corroded intermediate compression-bending H-section steel columns," *Engineering Structures*, vol. 308, Jun. 2024, doi: 10.1016/j.engstruct.2024.118025.
[25] ISO 15686-8:2008, "ISO 15686 (Service Life Planning)," 2008.
[26] Ad Straub, "Estimating the Service Lives of Building Products in Use," *Journal of Civil Engineering and Architecture*, vol. 9, no. 3, Mar. 2015, doi: 10.17265/1934-7359/2015.03.011.
[27] T. Potrč Obrecht, R. Kunič, S. Jordan, and A. Legat, "Roles of the reference service life (RSL) of buildings and the RSL of building components in the environmental impacts of buildings," in *IOP Conference Series: Earth and Environmental Science*, Institute of Physics Publishing, Sep. 2019. doi: 10.1088/1755-1315/323/1/012146.
[28] H. Sun, Y. Wang, J. Zhong, and K. Guan, "Failure Analysis of Corrosion Perforation of Heat Exchanger Plate," *Journal of Failure Analysis and Prevention*, vol. 25, no. 2, pp. 885–893, Apr. 2025, doi: 10.1007/s11668-025-02149-z.
[29] Z. Liu, W. Liao, W. Wu, C. Du, and X. Li, "Failure analysis of leakage caused by perforation in an L415 steel gas pipeline," *Case Studies in Engineering Failure Analysis*, vol. 9, pp. 63–70, Oct. 2017, doi: 10.1016/j.csefa.2017.07.003.
[30] B. T. Lu and J. L. Luo, "Correlation between surface-hardness degradation and erosion resistance of carbon steel - Effects of slurry chemistry," *Tribology International*, vol. 83, pp. 146–155, 2015, doi: 10.1016/j.triboint.2014.11.008.
[31] S. Shojai, F. Schönamsgruber, M. Köhler, and E. Ghafoori, "Impact of accelerated corrosion on weld geometry, hardness and residual stresses of offshore steel joints over time," *Materials and Design*, vol. 251, Mar. 2025, doi: 10.1016/j.matdes.2024.113578.
[32] R. Vera *et al.*, "Atmospheric corrosion and impact toughness of steels: Case study in steels with and without galvanizing, exposed for 3 years in Rapa Nui Island," *Heliyon*, vol. 9, no. 7, Jul. 2023, doi: 10.1016/j.heliyon.2023.e17811.
[33] B. Nie, S. Xu, and Y. Wang, "Time-Dependent Reliability Analysis of Corroded Steel Beam," *KSCE Journal of Civil Engineering*, vol. 24, no. 1, pp. 255–265, Jan. 2020, doi: 10.1007/s12205-020-1478-z.
[34] ISO, "ISO 12944 Paints and varnishes - Corrosion protection of steel structures by protective paint systems," 2018.
[35] S. J. Price and R. B. Figueira, "Corrosion protection systems and fatigue corrosion in offshore wind structures: Current status and future perspectives," *Coatings*, vol. 7, no. 2, Feb. 2017, doi: 10.3390/coatings7020025.
[36] C. M. Hewitt and AISC, "Design Guide 16 Assessment and Repair of Structural Steel in Existing Buildings," 2025.
[37] B. Zajec *et al.*, "Corrosion monitoring of steel structure coating degradation," *Tehnicki Vjesnik*, vol. 25, no. 5, pp. 1348–1355, Oct. 2018, doi: 10.17559/TV-20170206004112.
[38] M. Abbas and M. Shafiee, "An overview of maintenance management strategies for corroded steel structures in extreme marine environments," *Marine Structures*, vol. 71, May 2020, doi: 10.1016/j.marstruc.2020.102718.

In Press